# ChemComm

Accepted Manuscript


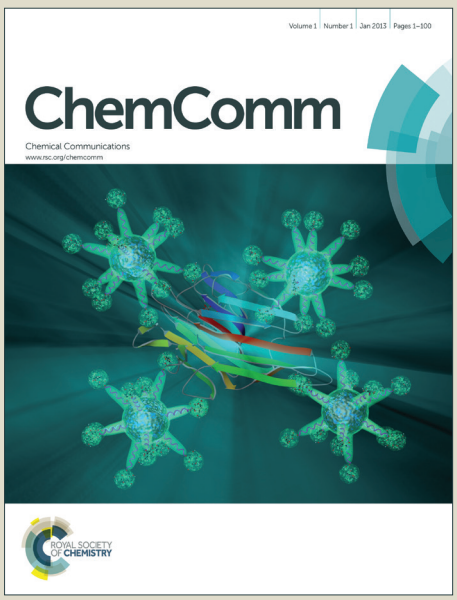





ROYAL SOCIETY OF CHEMISTRY

www.rsc.org/chemcomm

Journal Name

RSCPublishing

COMMUNICATION

# Application of graphene oxide as a hydrothermal catalyst support for synthesis of $TiO_2$ whiskers

Cite this: DOI: 10.1039/x0xx00000x

Kaushal R. Parmar,[a,b,c] Shaik Basha [a]* and Z.V.P. Murthy [b]*

Received 00th January 2012,
Accepted 00th January 2012

DOI: 10.1039/x0xx00000x

www.rsc.org/

**How Graphene Oxide (GO) with its step edges and wrinkles (~1-2 nm) acts as a catalyst in hydrothermal nucleation and growth is demonstrated. $TiO_2$ whiskers were prepared by using GO as a support while $TiO_2$ nanograss were prepared without using GO.**

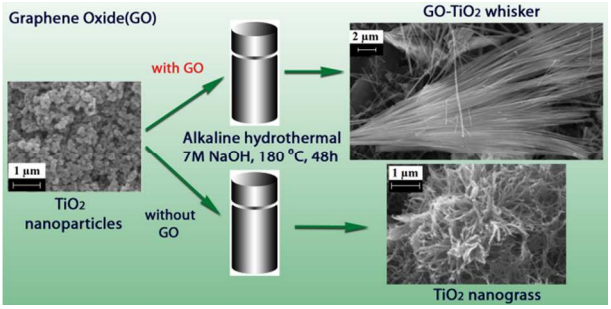


Scheme 1

Single layer sheet of carbon, Graphene, proved to be a wonder material due to its unique properties like excellent electron mobility at room temperature (200000 $cm^2$ $V^{-1}$ $s^{-1}$), very high theoretical (2500 $m^2$ $g^{-1}$) and experimentally measured (400-700 $m^2g^{-1}$) surface area, high Young's modulus (1 TPa) and optical transparency (97.7 %).[1] Graphene-based materials including graphene oxide (GO) are in constant research for their application in nanoelectronics, sensors, catalysts, contaminant removal, drug delivery, $H_2$ production and energy conversion. Among the various uses of graphene/GO, assembling other inorganic materials like metal or metal oxide nanoparticles/nanocrystals on graphene to fabricate composites or hybrids is in the focus.[2,3] Moreover, integrating graphene/GO with inorganic nanoparticles allows the properties of the nanocomposite to be engineered for specific applications. Attempts were made to enhance the properties of material by changing their morphology on the surface of graphene.[2,4]

Nanocrystalline titanium dioxide ($TiO_2$) with high-energy valence-band holes is extensively studied due to its potential applications in heterogeneous catalysis.[5] Due to its high chemical stability, nontoxicity and low cost makes $TiO_2$ biocompatible, and it is used as an alternative material for improving antimicrobial properties.[6] Owing to the attractive properties of nano-hybrids like graphene-$TiO_2$ composites, nanocrystal growth on graphene sheet is an important approach to produce them. Controlled nucleation and growth gives optimal chemical interactions and bonding between $TiO_2$ and graphene sheets, leading to the strongest electrical and mechanical coupling within the hybrid.[7] To date, there are only few reports on graphene-$TiO_2$ nano wire/rod composites.[2,8,9] Wang et al [10] showed that morphology of crystal can be controlled by tuning surface chemistry of graphene sheet.

As described above, many attempts were made to get different morphologies of metal oxides on graphene and/or GO, however, studies on effect of GO on morphological change is yet to be studied. In the present work, we are taking advantage of GO to not only enhance $TiO_2$'s properties but also use its step edges and wrinkles to guide the growth of titanate. We assembled $TiO_2$ whiskers on GO to produce GO-$TiO_2$ whisker composites without using any template. To the best of our knowledge, it is the first time that the GO-$TiO_2$ whisker composites are produced and this self-assembling procedure is facile and reproducible (Scheme 1).

Various oxygen groups like hydroxyl, carboxy, epoxy, alkoxy and carbonyl were observed in the FT-IR spectra of GO. (Fig. S1A, †ESI). The comparison between FT-IR spectra of pure $TiO_2$ powder, 10% GO-$TiO_2$ composite, 10% GO-sodium titanate whiskers and GO are shown in Fig. S1B (†ESI). Due to scale variation, comparison of 10% GO-sodium titanate whiskers and GO is done in separate figure for better understanding (Fig. S1C, †ESI). Almost all the functional groups of GO are present in GO-sodium titanate whiskers, however, they are significantly reduced due to hydrothermal reaction but did not disappear completely (Fig. S1C, †ESI). Detailed FT-IR analysis is available in †ESI.

The XRD pattern for sodium titanate nanograss and GO-sodium titanate whiskers after hydrothermal treatment with 7 M NaOH are shown in Fig. 1A. The formation of $Na_2Ti_nO_{2n+1}$ (n=3, 4, 9) was confirmed by the XRD due to hydrothermal reaction. Here in Fig. 1A, [1] [2] [3] correspond to peaks due to $Na_2Ti_3O_7$, $Na_2Ti_4O_9$ and $Na_2Ti_9O_{19}$.[11] Due to hydrothermal treatment with HCl, sodium ion is replaced by hydrogen to form hydrogen titanate ($H_2Ti_nO_{2n+1}$ where n=3, 4, 9) (Fig. 1B). Annealing at 450$^0$C converts hydrogen titanate in to photoactive forms.[12] Titanium nano grass consists of anatase $TiO_2$ and GO-$TiO_2$ whiskers consist of $TiO_2$ (B) which is also photoactive and their respective planes to corresponding peaks are

shown in Fig. 1B.[2,11,12] All the diffraction peaks can be readily indexed to monoclinic $TiO_2$ (B) phase (JCPDS 74-1940), and are in good agreement with the previous reports.[12] The diffraction patterns of graphite, graphene oxide and GO-$TiO_2$ whiskers after ion-exchange with HCl are presented in Fig. S2A and S2B (†ESI).

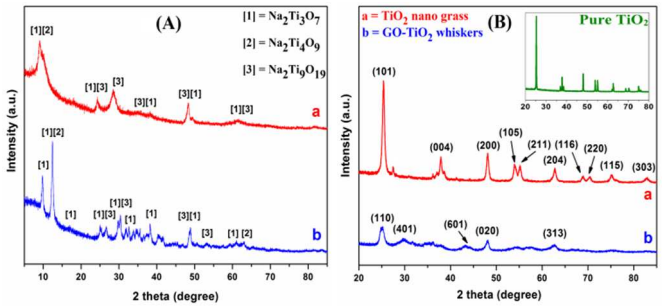


Fig. 1 XRD patterns: (A) composites before ion exchange with HCl and (B) composites after ion exchange.

Scanning electron micrographs of GO-$TiO_2$ composite prepared by sonication process are shown in Fig. 2a and S3 (†ESI). Here, $TiO_2$ nanoparticles are arranged on GO uniformly without any serious agglomeration. Figs 2a and S3 (†ESI) illustrate step edges and wrinkles of GO of several nanometers which play major role in nucleation and growth mechanism. These are the step edges and wrinkles from where $TiO_2$ whiskers start to grow. Fig. 2b-2d and S4 (†ESI) display sodium titanate nanograss obtained after alkaline hydrothermal reaction for 48 h. SEM observations reveal a large quantity of grass like nanostructures with typical widths, which are in nanometer scale (<50) (Table 1, †ESI). Significant change in the morphology was observed after addition of 10% GO (w/w) along with $TiO_2$ in the alkaline hydrothermal reaction. The structure of end product became whiskers shaped and named as GO-$TiO_2$ sodium titanate whiskers (Fig. 2b to 2h). This drastic change in morphology can be ascribed to GO. The sodium titanate whiskers had a width 100 to 250 nm and length 15-20 µm. Till-date, to the best of our knowledge, this type of morphology on GO surface was not observed in the literature. Fig. 2e, 2f display SEM images of GO-$TiO_2$ whiskers aged 48 h hydrothermally while Fig. 2g, 2h display images of composite aged 72 h. By these images, it can be observed that when the growth time is increased to 72 h, thickness of the $TiO_2$ nanorods increased. These rod-like structures undergo the dissolution-recrystallization process, namely, the well-known Ostwald ripening process.[13] Figure S5A, S5B (†ESI), which are at lower magnification, prove that all the material is converted into whiskers. Additional images of GO-$TiO_2$ whiskers (aged 72 h hydrothermally) are presented in Fig. S6A to S6E (†ESI).

Transmission electron microscopy was applied to investigate the microstructure of the composites, and the observed results are in agreement with XRD data. Figures 3a and 3b shows GO sheet and GO-sodium titanate whisker composite, respectively, and their corresponding selected area electron diffraction (SAED) are shown in the inset of figures. Individual rods of whisker can be seen on transparent graphene oxide sheet (Fig. 3b) and SAED pattern confirms that the sodium titanate whiskers are polycrystalline structures in nature and indicate that the growth of $TiO_2$ is along (001) plane, which is in consistent with XRD.

Figures 3c to 3f displays TEM images of GO-alkaline titanate whiskers before ion exchange for 48h hydrothermal time. Inset of Figure 3c shows SAED pattern of sodium titanate, which confirms its crystalline nature. Microscopy imaging (Figures 3e and S7A, †ESI) revealed the attachment of sodium titanate whisker to GO sheets, without detachment even under sonication conditions while preparing TEM sample. By measuring the lattice fringes and from the electron diffraction patterns taken along different zone axes (Figures 3d, 3f and S7B, †ESI) the lattice parameters were found to be in good agreement with XRD (d-spacing of 0.36, 0.73 and 0.34 nm corresponds 2Θ value of 25.01, 12.43 and 26.69°, respectively). Figures 3g, 3h, S7C and S7D (†ESI) shows TEM images of GO-$TiO_2$ whiskers after ion-exchange process. No morphology changes were observed due to HCl ion exhange however, changes in internal structure including a decrease in the average size and a narrowing of the size distribution was observed. High resolution TEM images are in good agreement with XRD as evidenced by d-spacing of 0.35 nm corresponds 2Θ value of 25.34°.

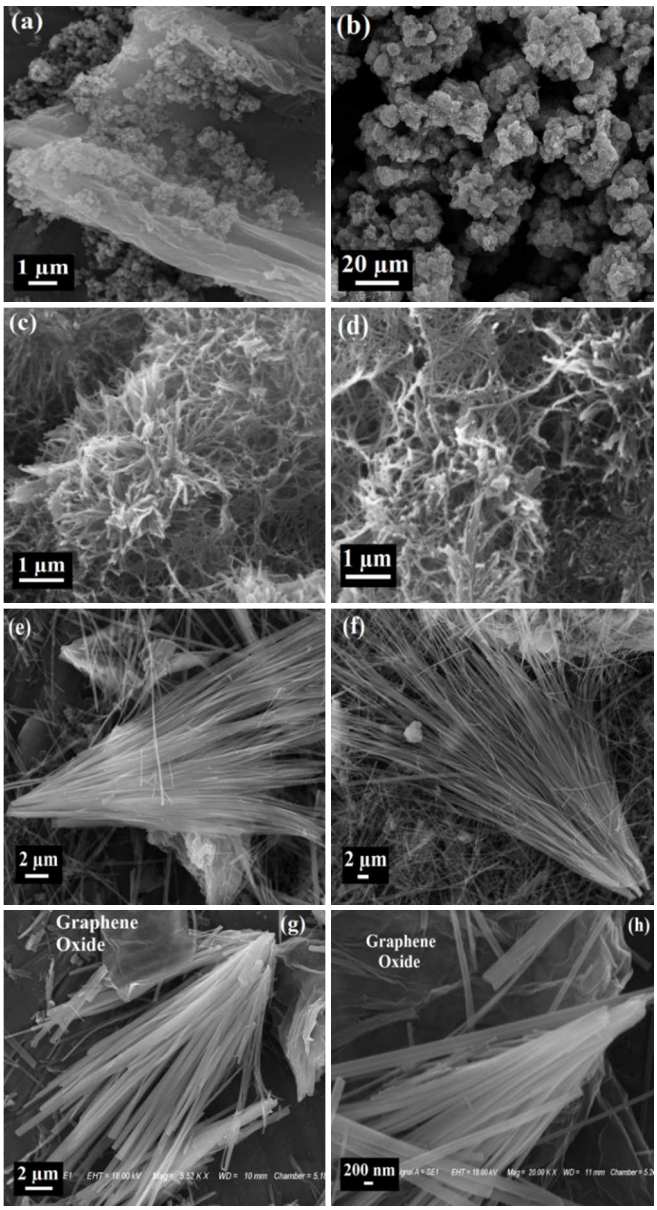


Fig. 2 SEM images: (a) GO-$TiO_2$ composite, (b, c, d) Sodium titanate nano grass (hydrothermal reaction, 48h), (e, f) GO- sodium titanate whiskers (hydrothermal reaction, 48 h), and (g, h) GO-sodium titanate whiskers (hydrothermal reaction, 72 h).

TEM images (Figures 3h to 3j) display crystalline morphology of as-prepared $TiO_2$ nanograss after ion exchange. The sample

mostly consists of polygonal cryatallites of sizes ranged from 10-15 nm. SAED image (inset of figure 3j) reveals a high crystallinity of the nanostructures, which was also confirmed by XRD. Watching nanograss' morphology closely one can conclude that the nanograss is consists on many polygonal highly crystalline nanoparticles. These nano crystallites are not oriented in any direction as seen in Figure 3g. TEM images of GO-$TiO_2$ composite (made by sonication process) can be seen in Figure S8 (†ESI). Figure S8B (†ESI) displays crystalline morphology of individual $TiO_2$ nano particle. By comparing high resolution TEM images of GO-$TiO_2$ composite (sonication) and nanograss we can conclude that nanograss is made up of many polygonal highly crystalline nano particles. Further we can compare this nanograss (after ion exchange) with pure $TiO_2$'s XRD pattern.[14]

The edge structures and competitive growth of nucleated cluster on GO are of particular importance as they govern the quality of the subsequent synthesized material.[15] Also, the GO surface interacts strongly with the coated species including $TiO_2$, due to higher density of oxygen functional groups including carboxylic, hydroxyl, and epoxy groups. These functional groups act as nucleation sites for $TiO_2$. However, the growth of nanoparticles is suppressed due to limited space between GO sheets defined by steric effect.[16] But in our case, the growth of $TiO_2$ on GO (GO- $TiO_2$ whiskers) was higher as compared to sodium titanate nanograss (Table 1, †ESI).

Here, we propose the mechanism as ***'step edge catalyzed cooperative growth of $TiO_2$.'*** $TiO_2$ nanoparticles trapped at wrinkles and step edges of GO where oxygen functionalities are present (Fig. 4). These edges act as nucleation sites and provide path during growth process. So, these nucleated clusters grow along with edges and may get separated. Due to cooperative growth, favourable nucleation sites and path, growth of $TiO_2$ is much faster. On the other hand, in pure $TiO_2$ (without GO) agglomerated form cannot nucleate fast enough due to non-availability of favourable nucleation sites.[17] On GO surface, where amount of $TiO_2$ is more, large whisker was formed while small whiskers were transpired at low concentrated area as confirmed by SEM. The width of a rod in whisker was increased with increase in hydrothermal time from 48 to 72 h. Dependence of nanostructure dimensions and morphology on the hydrothermal conditions supports that the phase transformation mechanism includes a dissolution-reprecipitation process.[18] A study to control the size and morphology of and size of $TiO_2$ particles is in progress. Additional information on whisker growth mechanism and related experimental evidences (i.e. immature $TiO_2$ whisker grown on GO) are provided in †ESI.

We report this whiskers type morphology of $TiO_2$ on GO for the first time that can be useful in many applications of such nanostructured materials. Main advantages associated with GO-$TiO_2$ whiskers include even distribution of $TiO_2$ on GO due to its shape, effective charge separation due to formation of schottky barrier between GO/graphene and $TiO_2$ whiskers,[19] energy savings in production of high L/D ratio $TiO_2$ due to catalytic effect of GO. The morphology of the nanocrystals formed on GO can be designed by the degree of oxidation of graphene and the reaction temperature, morphology of GO and the method could be extended to synthesize a wide range of functional nanomaterials.

In summary, we have successfully synthesized GO-$TiO_2$ whiskers and $TiO_2$ nanograss by a hydrothermal method. Alkaline hydrothermal experiments with and without 10% GO revealed drastic morphological changes of $TiO_2$ in which 10% GO was present. The hierarchical $TiO_2$ whiskers were assembled by the GO nanosheets with thickness ranged between 100-200 nm. The possible growth mechanism of $TiO_2$ whiskers on GO is proposed based on the experimental results. GO acts as a catalyst and its step edges and wrinkles as nucleation sites, which promote nucleation as well as growth. Furthermore, GO can be used as a hydrothermal support for not only $TiO_2$ but also for other metal oxides to obtain the desired morphology. This opens new direction for hydrothermal supports.

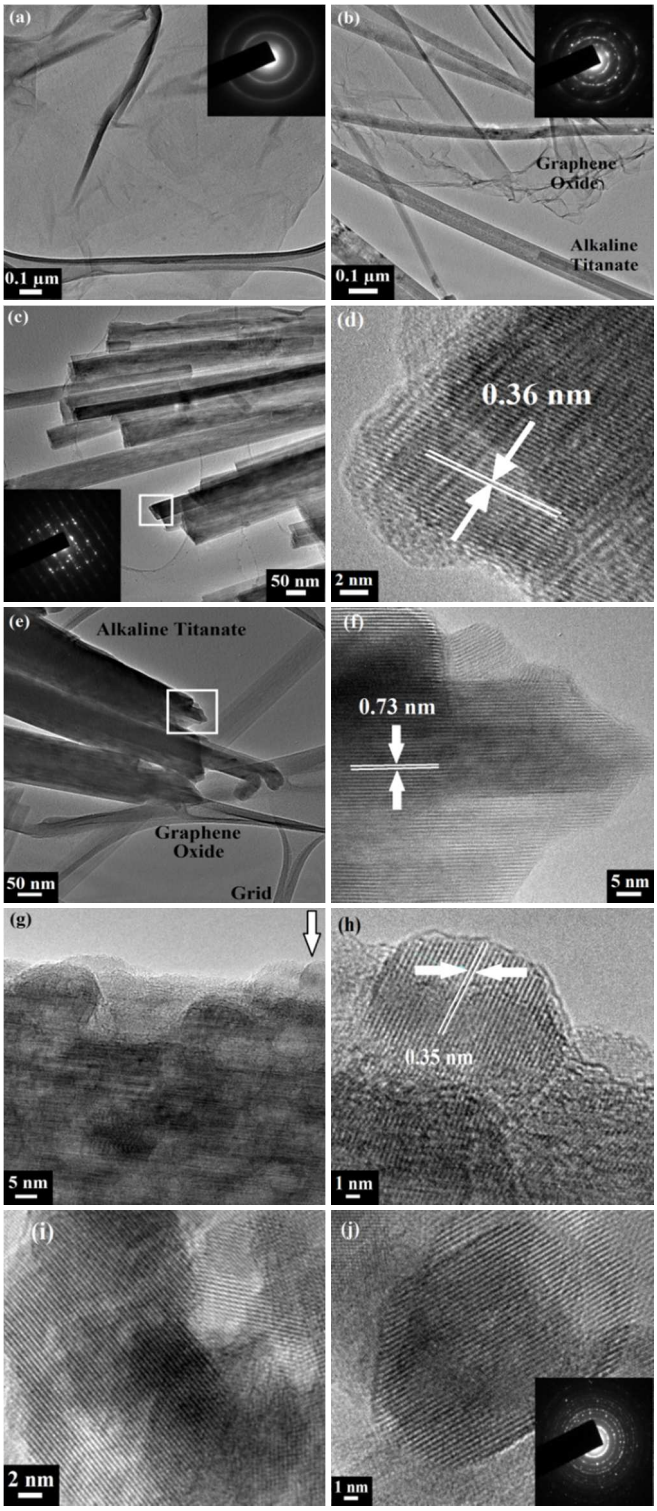


Fig. 3 TEM images (a) GO with SAED pattern; (b) GO-sodium titanate composite with SAED pattern; (c, e) sodium titanate whiskers at low resolution with SAED; (d,f) sodium titanate whiskers at high resolution; (g, h) GO-$TiO_2$ whiskers after ion exchange; (i, j) $TiO_2$ nanograss with SAED.

The morphology of the nanocrystals formed on graphene oxide can be tailored by the conditions including reaction time and the method could be extended to synthesize a wide range of functional nanomaterials. The as-prepared GO-$TiO_2$ whisker composites can be used in water treatment, Li-ion battery, dye sensitized solar cells and other optoelectronic applications.

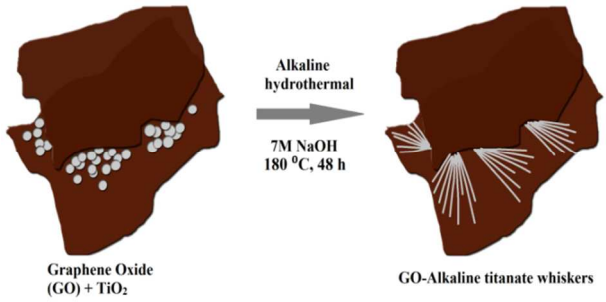


Fig. 4 Proposed mechanism for formation of $TiO_2$ whiskers on GO surface

The authors wish to express their sincere thanks to Prof. B. Jha, Discipline coordinator of Marine Biotechnology and Ecology and Dr. (Mrs) K.H. Mody, Group Leader, Marine Environment for their valuable suggestions. This is CSIR-CSMCRI contribution no. 132/2014.

## Notes and references

[a] Marine Biotechnology and Ecology Discipline
CSIR - Central Salt & Marine Chemicals Research Institute
Bhavnagar 364 002, Gujarat, India
[b] Department of Chemical Engineering, S.V. National Institute of Technology Surat, Surat - 395007, Gujarat, India.
* Corresponding Author. Tel.: +91 278 2561354; Fax: +91 278 2570885.
E-mail address: sbasha@csmcri.org (S Basha)
zvpm2000@yahoo.com (ZVP Murthy)
[c] Present address: Department of Chemical Engineering
Indian Institute of Technology Delhi, New Delhi – 110016, India

† Electronic Supplementary Information (ESI) available: [XRD, FT-IR, SEM and TEM images of various composites are available in the online version of this article.]. See DOI: 10.1039/c000000x/

1 (a) Xiang, Q.; Yu, J.; Jaroniec, M. Chem. Soc. Rev., 2012, 41, 782; (b) Zhu, Y.; Murali, S.; Cai, W.; Li, X.; Suk, J. W.; Potts, J. R.; Ruoff, R. S. Adv. Mater. 2010, 22, 3906.
2 Liu, J.; Bai, H.; Wang, Y.; Liu, Z.; Zhang, X.; Sun, D. D. Adv. Funct. Mater. 2010, 20, 4175.
3 (a) Xiang, Q.; Yu, J.; Jaroniec, M. J. Am. Chem. Soc., 2012, 134, 6575; (b) Xiang, Q.; Yu, J.; Jaroniec, M. Nanoscale, 2011, 3, 3670; (c) Dimiev, A.M.; Tour, J.M. ACS Nano 2014, 8, 3060.
4 (a) Luo, Q. P.; Yu, X. Y.; Lei, B. X.; Chen, H. Y.; Kuang, D. B.; Su, C. Y. J. Phys. Chem. C 2012, 116, 8111; (b) Wang, H.; Yang, Y.; Liang, Y.; Cui, L. F.; Casalongue, H. S.; Li, Y.; Hong, G.; Cui, Y.; Dai, H. Angew. Chem. Int. Ed. 2011, 50, 7364.
5 (a) Linsebigler, A. L.; Lu, G.; Yates, J. T. Jr. Chem. Rev. 1995, 95, 735; (b) Diebold, U. Surf. Sci.Rep. 2003, 48, 53.
6 Li, Q.; Mahendra, S.; Lyon, D. Y.; Brunet, L.; Liga, M. V.; Li, D.; Alvarez, P. J. J. Water Res. 2008, 42, 4591.
7 Lambert, T. N.; Chavez, C. A.; Hernandez-Sanchez, B.; Lu, P.; Bell, N. S.; Ambrosini, A.; Friedman, T.; Boyle, T. J.; Wheeler, D. R.; Huber, D. L. J. Phys. Chem. C 2009, 113, 19812.
8 (a) Huang, H.; Fang, J.; Xia, Y.; Tao, X.; Gan, Y.; Du, J.; Zhu, W.; Zhang, W. J. Mater. Chem. A 2013, 1, 2495; (b) He, L.; Ma, R.; Du, N.; Ren, J.; Wong, T.; Li, Y.; Lee, S. T. J. Mater. Chem. 2012, 22, 19061; (c) Pan, X.; Zhao, Y.; Liu, S.; Korzeniewski, C. L.; Wang, S.; Fan, Z. ACS Appl. Mater. Interfaces 2012, 4, 3944.
9 Perera, S. D.; Mariano, R. G.; Vu, K.; Nour, N.; Seitz, O.; Chabal, Y.; Balkus, K. J. Jr. ACS Catal. 2012, 2, 949.
10 Wang, H.; Robinson, J. T.; Diankov, G.; Dai, H. J. Am. Chem. Soc. 2010, 132, 3270.
11 (a) Lee, S. S.; Byeon, S. H. Bull. Korean Chem. Soc. 2004, 25, 1051; (b) Kolenko, Y. V.; Kovnir, K. A.; Gavrilov, A. I.; Garshev, A. V.; Frantti, J.; Lebedev, O. I.; Churagulov, B. R.; Tendeloo, G. V.; Yoshimura, M. J. Phys. Chem. B 2006, 110, 4030; (c) Nikolic, L. M.; Maletin, M.; Ferreira, P.; Vilarinho, P. M. Process. Appl. Ceram. 2008, 2, 109.
12 Armstrong, A. R.; Armstrong, G.; Canales, J.; Bruce, P. G. Angew. Chem. Int. Ed. 2004, 43, 2286.
13 Dong, W.; Li, B.; Li, Y.; Wang, X.; An, L.; Li, C.; Chen, B.; Wang, G.; Shi, Z. J. Phys. Chem. C 2011, 115, 3918.
14 Pol, V. G.; Langzam, Y.; Zaban, A. Langmuir 2007, 23, 11211.
15 Cai, C. J.; Xu, M. W.; Bao, S. J.; Ji, C. C.; Lu, Z. J.; Jia, D. Z. Nanotechnology 2013, 24, 275602.
16 Li, N.; Liu, G.; Zhen, C.; Li, F.; Zhang, L.; Cheng, H. M. Adv. Funct. Mater. 2011, 21, 1717.
17 Chen, X.; Mao, S. S. Chem. Rev. 2007, 107, 2891.
18 Hu, X.; Zhang, T.; Jin, Z.; Huang, S.; Fang, M.; Wu, Y.; Zhang, L. Cryst. Growth Des. 2009, 9, 2324.
19 Liu, B.; Huang, Y.; Wen, Y.; Du, L.; Zeng, W.; Shi, Y.; Zhang, F.; Zhu, G.; Xu, X.; Wang, Y. J. Mater. Chem. 2012, 22, 7484.



 